THIRD QUARTERLY REPORT

STUDY & DETERMINATION OF AN OPTIMUM DESIGN FOR SPACE UTILIZED LITHIUM DOPED SOLAR CELLS

15 April 1970

13154-6009-R0-00

R. G. Downing
J. R. Carter
W. K. Van Atta

Contract 952554

Jet Propulsion Laboratory
California Institute of Technology
Pasadena, California

TRW Systems Group
One Space Park
Redondo Beach, California 90278

THIRD QUARTERLY REPORT

STUDY & DETERMINATION OF AN OPTIMUM DESIGN FOR SPACE UTILIZED LITHIUM DOPED SOLAR CELLS

15 April 1970

13154-6009-R0-00

Prepared by:

R. G. Downing

Approved by:

J. L. Rogers

Contract 952554

Jet Propulsion Laboratory
California Institute of Technology
Pasadena, California

TRW Systems Group
One Space Park
Redondo Beach, California 90278

This work was performed for the Jet Propulsion Laboratory, California Institute of Technology, as sponsored by the National Aeronautics and Space Administration under Contract 952554.

TABLE OF CONTENTS

LIST OF ILLUSTRATIONS

LIST OF ILLUSTRATIONS (Cont.)

ABSTRACT

Recently Hall coefficient measurements have been made on lithium-doped float-zone silicon which has dopant concentrations comparable to those found in solar cells. The results of the measurements of these materials indicate that two defect complexes are formed during irradiation. The Si-A center (oxygen-vacancy pair) is one of these defects. The other defect is associated with deeper lying energy and may be a lithium-vacancy pair. Capacitance measurements on lithium-doped quartz-crucible solar cells have been made as a function of voltage and frequency. This work indicates that the irradiation of this type of solar cell results primarily in the formation of Si-A centers. These defects are later annihilated by reaction with lithium donors. Lithium was diffused into p-type silicon to form lithium compensated p-type silicon with resistivities in practical device range. Lithium compensated p-type silicon has been irradiated and the electrical measurements suggest that lithium reacts with radiation defects in a manner which may provide an additional hardening effect in n on p solar cells. A study was done to evaluate the effectiveness of bismuth and tin doping to achieve radiation hardness. The results were negative.

The solar cell evaluation program shows continued improvement in the fabrication of high efficiency radiation resistant lithium-doped cells. Additional evidence has been acquired indicating the superiority of longer time lower temperature diffusion schedules in producing higher pre-irradiation and post-annealing solar efficiencies. Solar simulator measurements on several of the better groups clearly show the superior radiation resistance of lithium-doped p/n cells relative to the contemporary 10 ohm-cm n/p cell following exposure to 3×10^{15} e/cm^2 1 MeV electrons and annealing.

I. KINETICS OF LITHIUM IN SILICON

The past quarter's efforts have again been concentrated on obtaining additional data to support a physical model for the damage and recovery processes in lithium solar cells. Considerably more data has been gathered to support the proposed model for lithium cells made from quartz-crucible silicon. In addition, more information has been developed regarding the nature of radiation defects in lithium-doped float zone silicon. A new phase of research has been opened in regard to use of lithium in radiation hardening. This work has involved the preparation of p-type silicon which is effectively counterdoped with lithium. The initial evaluations of this material under particulate radiation indicates that the lithium may provide a hardening effect in p-type silicon. An evaluation program was also completed regarding the effect of other dopants in achieving some degree of radiation hardness.

A. Hall Coefficient Measurements

Our previous Hall coefficient measurements on lithium-doped float zone silicon have been concentrated on heavily doped specimens. These heavy doping levels are not typical of those found in solar cells. To extend the previous work, float-zone specimens were prepared with lithium concentrations in the range of $10^{14}/cm^3$ to $10^{15}/cm^3$. The float-zone silicon used for this work was originally 1000 ohm-cm n-type silicon. This purity level restricts the possible defect interactions with impurities to those with lithium and possibly oxygen. Sample E-4 is an example of such a specimen. The Hall coefficient data relating to the irradiation and recovery of this sample is shown in Figure 1. Since the reciprocal Hall coefficient is closely related to the conduction band carrier concentration, the results in Figure 1 can be interpreted as changes in carrier concentration. The results of the irradiation similar samples of quartz-crucible silicon show a very small carrier concentration change at room temperature after irradiation. Those results support the production of Si-A centers (oxygen-vacancy pairs) during irradiation of the lithium-doped quartz-crucible silicon. Two significant points can be observed regarding the after-irradiation results of sample E-4. First, the carrier removal at

room temperature is approximately 0.1 cm^{-1}. The second point is the large inflection in the Hall coefficient at temperatures at which the Fermi level is near 0.17 eV below the bottom of the conduction band. Although alternate explanations can be proposed, the simplest model would be the formation of two types of defects during the irradiation; one defect being the Si-A with ionization energy of 0.17 eV and a second defect being defect of undetermined structure with an ionization greater than 0.3 eV from the conduction band. The second defect is probably a lithium-vacancy pair. The introduction rate of the Si-A center in this sample appears to be approximately 0.2 cm^{-1}. The value is in excellent agreement with that found in similar quartz-crucible silicon. It is important to note that this sample contains only 3.7×10^{14} lithium donors/cm^3. Since the residual oxygen concentration in float-zone silicon is believed to be in the range of $10^{15}/cm^3$, oxygen is probably the dominant impurity in a float-zone specimen such as E-4. In this regard it is not unusual that the Si-A center should be produced during irradiation. After irradiation the sample was stored at room temperature to study recovery changes. After 310 hours at 26°C, the carrier concentration was greatly reduced during storage. At this time the decline of the reciprocal Hall coefficient at temperatures below room temperature indicates that many shallower level defects (i.e., Si-A centers) remain in the sample. After 1500 hours the conduction electron concentration has been reduced to only a few percent of that present immediately after the irradiation. It appears that the time dependent decrease of carrier concentration is directly related to the reaction of lithium donor ion cores and their attendant electrons with radiation defects.

A similar specimen, F-2, with a somewhat higher lithium concentration, was studied in the same manner. The results of the this study are shown in Figures 2 and 3. In this sample, the concentration of lithium donors was $1.5 \times 10^{15}/cm^3$. This is roughly four times the amount present in sample E-4. The float-zone silicon used in samples E-4 and F-2 was purchased from the Wacker Chemical Corp., Los Angeles. Figure 2 shows the reciprocal Hall coefficient versus reciprocal temperature plot for sample E-2 before irradiation, after irradiation, and 800 hours after irradiation. To facilitate easy interpretation of this data, it was

normalized to the before irradiation results and replotted on a linear scale in Figure 3. The features of the change produced by irradiation of this sample are very similar to those shown in Figure 1 for sample E-4. The presence of both the Si-A center and the defect with a deeper level are implied after the irradiation. The introduction rate for Si-A centers in sample F-2 is approximately 0.2 cm^{-1}. This is the same as that found in sample E-4. It is also the same as that found in a quartz-crucible sample (Q-2C, previous quarterly) with similar lithium concentrations. The one significant difference between the results in sample F-2 and those in sample E-4 is the introduction rate of defect with deeper energy is about 0.2 cm^{-1} in former and 0.1 cm^{-1} in the latter case. It would appear that increased lithium concentrations cause higher concentrations of the subject defect to be formed during irradiation. Because of mass action principles, this increased introduction rate is direct evidence that lithium is involved in the structure of the defect under consideration. After 800 hours at room temperature, the results in Figure 3 indicate greatly reduced carrier concentration. The data also indicates a very much reduced concentration of defects with energy levels less than 0.32 eV (i.e., Si-A centers).

B. Capacitance Measurements

The previous quarterly discussed the use of capacitance measurements to monitor the internal changes in lithium concentration as a function of distance from the space charge region during irradiation and recovery. In the intervening period a group of lithium-doped solar cells was received from JPL for evaluation. These showed significantly superior characteristics and a complete capacitance study was made to detect any possible differences which would account for the behavior. In Figure 4 data for cell number H2A7249 is shown. This cell was fabricated from quartz-crucible silicon. The calculated donor concentrations are plotted in Figure 4 as a function of barrier width. Data is plotted for the before and after irradiation conditions and after recovery. The electrical output characteristics of this of this cell are noted on the figure and will be discussed in other portions of this report. The outward appearances of the data in Figure 4 is very similar to that of other quart-crucible cells

studied (AF 14-4912, previous quarterly). In general a very small decrease in net donor concentration occurred during irradiation. During recovery, however, a large decrease of donor concentration occurs. These changes are shown more clearly in Figure 5. In this figure the removal rates during irradiation and recovery are plotted for various distances from the space charge region. The removal rate during irradiation is about 0.005 cm^{-1} and independent of distance from the space charge region. The removal rate during recovery is 0.08 cm^{-1} at the edge of the space charge region and rises rapidly to about 0.3 cm^{-1} at a distance 2 microns farther into the cell. As explained in the previous quarterly, the low removal rate during irradiation is consistent with Si-A center formation during irradiation. The removal is low because only a few percent of these defects are ionized at room temperature. The actual introduction of Si-A centers implied by the observed removal rate is about 0.2 cm^{-1}. It is interesting to note that the removal rate during recovery is observed to go as high as 0.3 cm^{-1} and the trend of the data indicates that it continue to go higher. These results tend to support a model in which more than one lithium atom reacts with each Si-A center during the recovery. Another fact of interest about this cell is that a significant lithium concentration remains after recovery. This is illustrated by the fact that donor concentrations after recovery, in Figure 4, are still well above the phosphorus concentration. These higher concentrations allow sufficient lithium for the annihilation of radiation defects without exhausting the lithium near the junction. If exhaustion of the lithium occurs, the recovery will not proceed to completion.

Since the result of the capacitance measurements of removal rates during irradiation of lithium-doped quartz-crucible cells strongly indicates that Si-A centers are formed, it would be interesting to examine similar measurements made on conventional p on n solar cells. The silicon "A" center is believed to be the major recombination center in the conventional p/n solar cell (quartz crucible silicon). In Figure 6 the donor concentrations, determined by capacitance measurements, are shown for a non-lithium solar cell (CEG 112) as a function of distance into the n-type base region. The measured carrier removal rate is constant throughout the distance investigated with a value of 0.13 cm^{-1}. Under the conditions in this cell,

Si-A centers would be about 9% ionized. The actual introduction rate of "A" centers would be 0.15 cm^{-1}. This value is quite close to the value of 0.2 cm^{-1} which is calculated from similar measurements on lithium-doped quartz crucible solar cells. This result tends to support the previous conclusions that oxygen-vacancy pair (Si-A centers) play a prominent role in the degradation process of all p/n silicon solar cells.

In our previous final report, the possibility of using the frequency dependence of solar cell capacitance in the study of radiation defects was explored. This technique has recently been used to study lithium solar cells. The results of this experimentation appear to be very significant, and should provide an excellent means of study in the future. In this measurement the region of the solar cell space charge region is caused to widen and contract under a high frequency voltage. When deep lying energy levels are present, under certain conditions of frequency and temperature, these defects are not able to change their charge state rapidly enough by thermal emission and capture as the space charge region passes through their position. This difficulty provides a relaxation effect which can be studied to determine the energy levels of defects present. This behavior is illustrated by the data in Figure 7. In this work lithium-doped quartz-crucible silicon solar cells were studied in the unirradiated and irradiated conditions by capacitance measurements at temperatures from 27°C to -190°C and frequencies of 5 KHz to 400 KHz. In the case of a typical lithium-doped solar cell the donor concentration at the edge of the space charge is related to the capacitance in the following expression:

$$N_D = \frac{S\ V\ C^2}{q \cdot \varepsilon}$$

All of the factors in this expression are constant before and after irradiation except S, which is related to exponent of the $k = VC^n$ relationship of the cell. In this case the "S" factor was observed to be unchanged by irradiation. For this reason changes in donor concentration caused by irradiation can be studied by examining the changes in the square of the ratio of capacitance after irradiation to that observed before irradiation. This parameter is plotted on the ordinate of Figure 7. Examination of the data indicates that at higher temperatures no frequency dependence is observed.

As the sample temperature is reduced a divergence in the data for various frequencies is observed. The lower frequency (5 KHz) capacitance values diverge first as the sample temperature is decreased, followed by those of higher frequency at still lower temperatures. At -190°C (1000/T=12) the capacitance variation with frequency again converges. The behavior in general is indicative of deep lying traps produced by the electron irradiation. The point at which the transition from maximum to minimum donor population is half complete is marked for each frequency used. This point is defined as the cutoff frequency at that particular temperature. It can be assumed that the reciprocal of the cutoff frequency is proportional to the relaxation time of the electronic capture process dominating the process.

$$\tau = k \frac{1}{f_c}$$

The relaxation time of such processes can be determined from statistical considerations. In a case which can be described as a net loss of donors, the expression would be

$$\tau = 1/C_n N_c \exp [-\Delta E/kT]$$

where: N_c = the effective density of state
C_n = capture constant for electrons

To facilitate the analysis we have assumed the reciprocal of the cutoff frequency is equal to the relaxation time. To determine the energy level of the centers involved in the relaxation (ΔE), an activation energy plot is presented in Figure 8. In order to construct a plot in which the slope will directly reflect the value of ΔE, the relaxation time divided by the density of states is plotted versus the reciprocal temperature. The data indicates the value of ΔE to be 0.17 eV. Since this value is also identified with the ionization energy of the Si-A center, these measurements add more support to previously discussed evidence indicating that the primary defect produced during irradiation of lithium-doped quartz-crucible silicon solar cells is the oxygen-vacancy pair or Si-A center. Certain factors such as spin degeneracy, temperature dependence of capture crossection, and width of the space charge region have been neglected in this analysis. It is believed that consideration of such factors would not significantly alter the conclusions.

C. Lithium Counterdoping of p-Type Silicon

The benefits of radiation hardening by lithium doping have been so far confined to n-type silicon. This is an unfortunate circumstance, as n-type silicon is inherently more prone to displacement type radiation damage than is p-type silicon. Lithium doping has made n-type silicon competitive and in some cases superior to p-type silicon in regard to radiation hardness. A much more desirable situation would be to further increase the radiation hardness of p-type by lithium or any other type of doping. In an effort to determine if any such advantage does in fact exist, we have fabricated p-type silicon which is counterdoped by the diffusion of lithium. The results of electrical measurements made on a few p-type lithium counterdoped samples are summarized in Table 1. Two of these samples were made with quartz-crucible silicon and the other from float-zone silicon. In all cases the resistivity after lithium diffusion is much higher than the original resistivity of the crystal. This is evidence that many of the boron donors originally present in the crystals have been compensated by the presence of the lithium donors. This compensation was also confirmed by Hall coefficient measurements. The boron and lithium concentrations shown in Table 1 were determined in this manner. The Hall mobility of each specimen after the lithium diffusion is also shown. It can be noted that the mobilities shown are relatively low for samples of the resitivities exhibited after lithium diffusion. This is because mobility reflects the total concentration of scattering centers (i.e., both boron and lithium ion cores). The mobilities shown are more typical of the original crystal, since the possible scattering center population has been increased although the net carrier concentration in the valence band has been decreased. For this reason a lithium compensation diffusion of a p-type crystal will raise the Hall coefficient and decrease the Hall mobility. A large decrease in mobility may not be detected because of pairing of the lithium and boron atoms. The significant point is that p-type silicon can be lithium counterdoped to achieve resistivities of interest to the device designer and lithium concentrations which could be of importance in radiation hardening.

In an effort to obtain some indication as to possible hardening mechanisms, the p-type lithium-doped silicon samples discussed in Table 1 were irradiated with 1 MeV electrons. In this work only the Hall coefficients and resistivity were monitored. In this way any radiation induced reactions which affect majority carrier behavior can be detected. Although this does not measure the minority carrier lifetime, similar measurements in n-type reflect the reaction of lithium with the radiation generated defect complexes. In Figure 9 the hole concentration of sample Li-P-Q.C.-1-1 is plotted versus electron fluence. After an irradiation of 3×10^{16} e/cm^3 the sample was stored at 100°C. The slightly elevated temperature was used because of the known reduction of effective diffusion constant of lithium in quartz-crucible silicon. As shown in Figure 9 the hole concentration was significantly increased during the storage at 100°C. Since defects in p-type silicon do not normally anneal at this temperature, it appears that lithium may have reacted with some of the defects generated during the irradiation to annihilate them. In this p-type of sample, a decrease in lithium donors causes the hole concentration to increase because of the lowered compensation. These results are by no means conclusive, but do indicate that further work is warranted.

The data shown in Figure 10 relates to a similar sample which was lithium counterdoped to a much higher resistivity (Li-P-Q.C.-10-4). In the sample the removal rate during irradiation was 0.03 cm^{-1} which is similar to that of ordinary boron-doped silicon. In this sample the hole concentration also increased during storage at 100°C. The initial increase was larger than that of the previous sample; however, after 40 hours at 100°C the hole concentration decreased to less than that observed after the irradiation. The nature of this change is not clear at this time.

The data in Figure 11 represents the only study to date on p-type lithium counterdoped float zone silicon (Table 1). This material is of interest, in this case, because of the lower oxygen concentration. This lower oxygen concentration may allow any lithium reactions occurring to be observed in a shorter period of time at room temperature. In Figure 10 the hole concentrations before and after irradiation are plotted on the ordinate of the graph. The hole concentrations at various times after completion of the irradiation are shown in the figure. It is apparent

that after the decrease of hole concentration caused by irradiation, a large time dependent increase in hole concentration occurs. The hole concentration reaches a maximum of 40 hours after irradiation and then declines somewhat from the maximum. The magnitude of the hole increase observed with time is much greater than that of the decrease which occurred during irradiation. It is difficult to give a full explanation of these effects on the basis of this limited work. It does appear that in some way, irradiation of this material initiates a time dependent reaction, probably involving lithium donors, which results in a very significant increase in the hole concentration. Because of equilibrium considerations involving boron, this loss of donors can not be explained as a simple precipitation of lithium. In view of the known behavior of annihilation of recombination centers in n-type, the behavior observed in p-type lithium compensated silicon strongly suggests that similar reactions between lithium and recombination centers may also occur in p-type silicon. If this is in fact the case, the development of lithium-doped n on p solar cells with a highly superior radiation resistance may be within practical achievement. Further work in this area appears to be warranted.

D. Other Impurities

We have previously evaluated silicon doped with larger substitutional atoms in regard to a possible radiation hardening mechanism. In previous work, a single crystal silicon - 13% germanium alloy - was grown by the quartz crucible technique. This alloy crystal was doped with boron in the usual manner to produce an 8 ohm-cm p-type crystal. This material was fabricated into solar cells and evaluated for radiation resistance. The cells produced from this alloy were satisfactory in regard to photo output, but proved to be more prone to radiation damage than conventional n on p cells. The basis for this work was as follows. The vacancies produced by the energetic particles are surrounded by a tensile strain field. Substitutional atoms larger than silicon atoms are surrounded by a compressive strain field. If radiation produced vacancies could be trapped by large substitutional atoms, due to the lowering of their collective strain energy, the vacancies would be prevented from forming complexes which are recombination centers. This logic is in error in the

case bismuth since a vacancy trapped next to a bismuth atom is simply a Si-E center (i.e., a possible recombination center). In the case of germanium the strain field is limited because that atom is only 3% larger than silicon.

Our current effort involved two silicon crystals doped with larger substitutional atoms. Both crystals were grown from quartz-crucibles. One crystal was n-type silicon doped with bismuth to a resistivity of 0.5 ohm-cm. The other crystal was a p-type silicon - 0.5% tin alloy doped with boron to 20 ohm-cm.

We are indebted to Peter Iles of Centralab Semiconductor Division who fabricated several wafers of these two crystals into solar cells for evaluation. The two groups of cells were evaluated by monitoring the short circuit current with a one sun equivalent of tungsten illumination, during a 1 MeV electron irradiation. The data from this work is presented in Figure 12. The behavior of typical p/n and n/p solar cells are also shown as dashed lines in Figure 12. The short circuit currents of the bismuth cells (2,5) are slightly higher during irradiation than that of a comparable p/n cell. This difference does not appear to be of any practical significance. In the case of the silicon-tin alloy cells (A4, B2), they appear to degrade under electron fluence well before the comparable n/p cells which are in common use today. In view of these results it must be concluded that little or no practical hardening advantage can be achieved by addition of large substitutional atoms to the silicon lattice. In fact the addition of the large neutral substitutional atoms to p-type silicon appears to promote the formation of more or more effective recombination centers. No further work is planned in this area.

II. LITHIUM SOLAR CELL EVALUATION

A. New Cell Group Evaluation

The recovery characteristics of the most recent groups of cells, H3A (325/480), H9 (425/90/60), and H10 (425/90/60), have been determined as a function of time and temperature after irradiation with 1 MeV electrons and compared with the best of previous cell groups. A brief summary of the comparison is presented here separately for the crucible and float zone base material. The best prior groups of crucible cells annealed at 100°C are shown in Table IV. Although the H14 group was not constructed specifically for this program, it represents one of Heliotek's better crucible groups and is included here for comparison purposes. The two new groups, H10 and H3A, exhibited recovery levels of 38-40 ma and 40-41 ma, respectively, with half-annealing times of 1 hour at 100°C. In addition, the H3A group exhibited higher initial outputs than any prior group of lithium doped cells tested to date which possessed annealable characteristics. As indicated, the recovered short circuit current levels are slightly lower for the latter groups compared to the best prior data which were represented by the T2 and T7 groups; however, the H3A group exhibited less curve factor degradation and to date less redegradation effects than the prior groups, which would indicate overall superiority in terms of preservation of maximum power output. It is of interest to note that the longer time, lower diffusion temperature groups are continuing to exhibit characteristics competitive with or better than the best of the shorter time, higher diffusion temperature groups.(See Tables II-IV, Figs. 13-16).

A similar comparison can be made for the recovery characteristics at room temperature of float zone lithium doped cells. As in the previous comparison, all of the groups of cells were not directly associated with this particular contract, but are included as being representative of the state-of-the-art. The best yet groups are shown in Table IV. The new groups now under study are H9 (425/90/60) with maximum recovered level of 38 ma in half-annealing time of 5 hours. Although we have not yet tested any recent long time, low temperature diffused float zone lithium cells, there appears to be a measurable difference, though slight, in the superiority of the 120 minute redistribution over the 60 minute redistribution.

The new groups of cells have not to date exhibited any detrimental curve factor decay or redegradation. (See Tables II-IV, Figs 17-18).

Several trends seem to be evident in the summary presented above of cells fabricated over the last two years. First it appears that the 325°C, 480 minute diffusion consistently produces cells which are equal to the best produced with the higher temperature, longer time diffusion, whereas the average response over all the cells produced with the latter diffusion schedule is considerably poorer and widely variant. Other variables, such as initial resistivity, paint-on versus evaporated source, inclusion of an N^+ layer, and variation of parent dopant do not seem to have measurable or significant effects on overall cell performance. Finally, annealing rates of the more recent cells appear to be consistent with previous data as shown in Figure 19 for the H3A and H10 crucible cell groups. The activation energies for annealing appear to be consistent with the 1.10 eV slope anticipated for oxygen rich crucible material.

B. Solar Simulator Measurements

The majority of the I-V curves obtained in the evaluation program have been obtained using tungsten illumination because of its convenience, reliability, and amplification of radiation induced degradation. In addition, the majority of the annealing data has been taken at the short circuit current point. Although most cell groups exhibit stable I-V characteristics allowing qualitative linear comparisons for anticipated responses, under solar simulation, the quantitative magnitude of the annealing performances under solar simulation is difficult to extrapolate for the lithium cell. For these reasons, solar simulator measurements have been performed on a selected number of cell groups which are representative of the most superior lithium doped p/n cells evaluated to date. The pre-irradiation, post-irradiation, and after-annealing maximum power points have been plotted in Figure 20. The annealing rate curves shown are the same as those observed under tungsten illumination and are assumed to have been the same under solar simulation. As is indicated in the curves, the pre-irradiation initial effeciencies are competitive with contemporary n/p solar cells and the annealed outputs are in every case superior to the contemporary n/p cell after 3×10^{15} e/cm^2. There is, however, a wide divergence

in annealing rates which is probably due to differences in oxygen concentration among the various groups. It is of interest to note that of the three groups presented, two of them were fabricated utilizing the slower 325°C/480 minute diffusion schedule. This data confirms that significant progress has been made in the last several years in the generation of a technology to manufacture high efficiency stable lithium doped p/n cells which exhibit superior radiation resistance after annealing relative to the contemporary 10 ohm-cm n/p cell.

III. PROGRESS IN THE NEXT REPORT PERIOD

During the next report period the work on frequency dependent capacitance measurements will be continued and extended into lithium-doped float-zone solar cells. The work on p-type lithium compensated silicon will be continued and attempts will be made to study the changes in minority carrier lifetime during and after irradiation of this material. The solar cell evaluation program will be completed for all JPL furnished cells received during the contract period.

IV. NEW TECHNOLOGY

There is no new technology reported for this quarter.

V. PAPERS AND PUBLICATIONS GENERATED

Accepted for Publication

Title: "Effect of Electron Irradiation on Lithium-Doped Silicon"
Journal: International Journal of the Physics and Chemistry of Solids.

Accepted for Presentation

Title: "Role of Lithium in Irradiated Solar Cells"
Meeting: International Colloquium on Solar Cells, Toulouse, France, 6 July 1970.

Submitted for Consideration

Title: "Role of Lithium in Irradiated Solar Cell Behavior"
Meeting: Eighth Photovoltaic Specialists Conference, Seattle, Wn., 11 August 1970.

TABLE I. SUMMARY OF P-TYPE LITHIUM COUNTERDOPED SAMPLES

Sample	Orig. Crystal	Boron Conc.	Lithium Diff. Crystal	Lithium Conc.	Hall Mobility
Designation	Type, resistivity	atoms/cm^3	Type, resistivity	atoms/cm^3	cm^2/volts sec.
Li-P-Q.C.-1-1	p, 0.1 ohm-cm, Q.C.	$8x10^{17}$	p, 1.3 ohm-cm	$4x10^{17}$	175
Li-P-Q.C.-10-4	p, 1.8 ohm-cm, Q.C.	$8x10^{15}$	p, 26 ohm-cm	$7.5x10^{15}$	290
Li-P-F.Z.-10-3	p, 1.5 ohm-cm, F.Z.	$1x10^{16}$	p, 8 ohm-cm	$0.8x10^{16}$	300

TABLE II. LITHIUM SOLAR CELL MANUFACTURING PARAMETERS

Cell Group	Base Material			Lithium Introduction	
	Type	Dopant	Resistivity Ω-cm	Diff. Sched. °C/Min/Min	Li Concentration at junction cm^{-3}
H9	F.Z.	P	20	425/90/60	1.2 to 10.5 x 10^{14}
H10	Cruc.	P	20	425/90/60	2.2 to 6.3 x 10^{14}
H3A	Cruc.	P	20	325/480	0 to 4.1 x 10^{14}

TABLE III. LITHIUM SOLAR CELL RECOVERY CHARACTERISTICS AFTER 3 x 10^{15} e/cm^2, 1 MeV

Cell Group	Average N_{Li} cm^{-3}	Annealing Temp	Initial Level I_{SC},ma	Damaged Level I_{SC},ma	Recovered Level I_{SC},ma	Time to 1/2 Recovery Point (hours)
H9	9x10^{14}	25	45	22	38	5
H10	4x10^{14}	100	54-58	22-24	38-40	1
	4x10^{14}	60	49-55	22	38-40	30
H3A	3x10^{14}	100	52-64	21-27	40-41	2
	3x10^{14}	60	53-61	22-27	38-42	70
	2x10^{14}	25	59	23-25	---	--

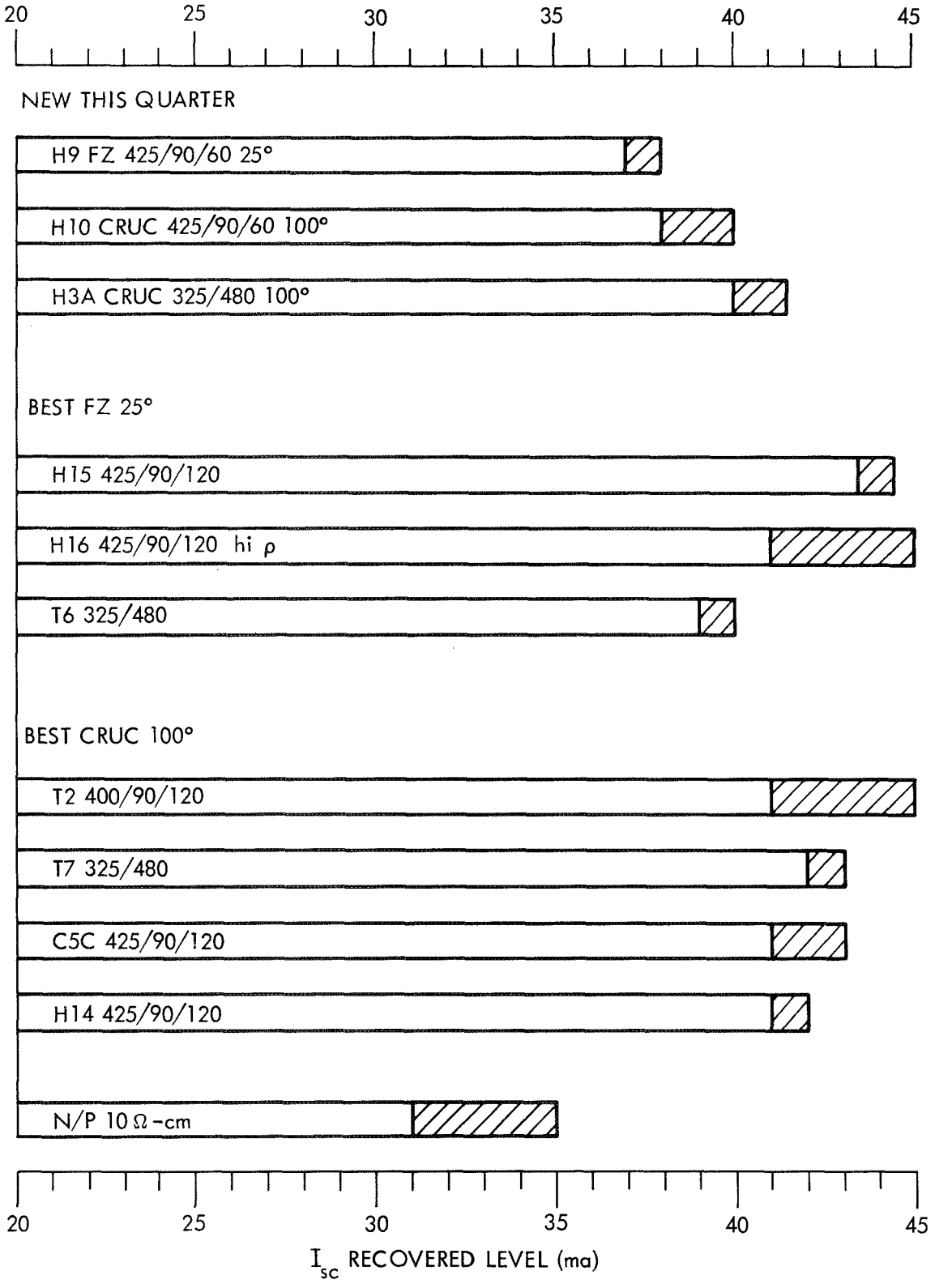

TABLE IV. COMPARISON OF PEAK RECOVERED LEVELS (I_{SC}-TUNGSTEN)

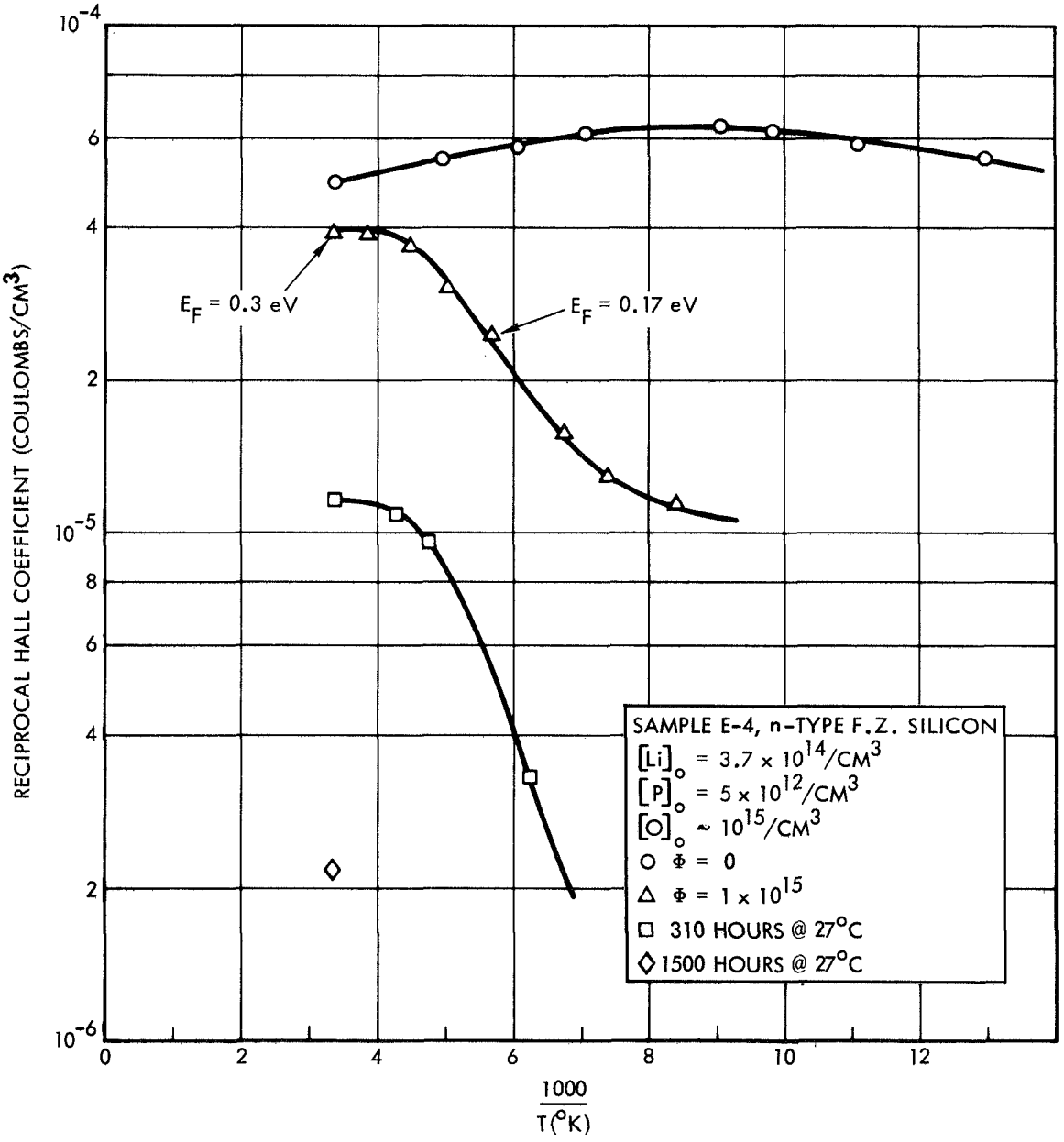

FIG. 1 HALL COEFFICIENT VS TEMPERATURE, IRRADIATED LI-DOPED FLOAT ZONE SILICON

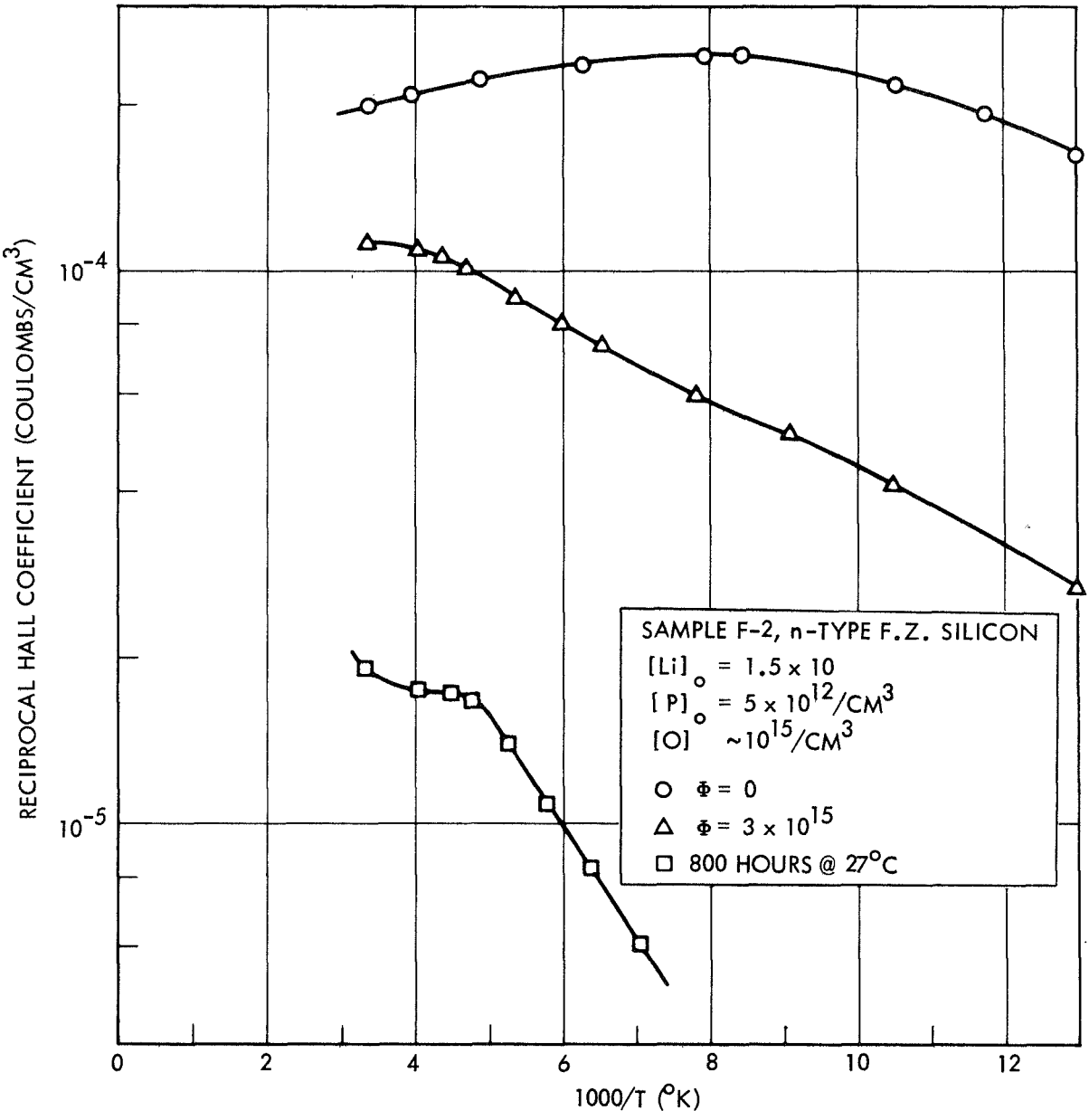

FIG. 2 HALL COEFFICIENT VS TEMPERATURE, IRRADIATED LI-DOPED FLOAT ZONE SILICON

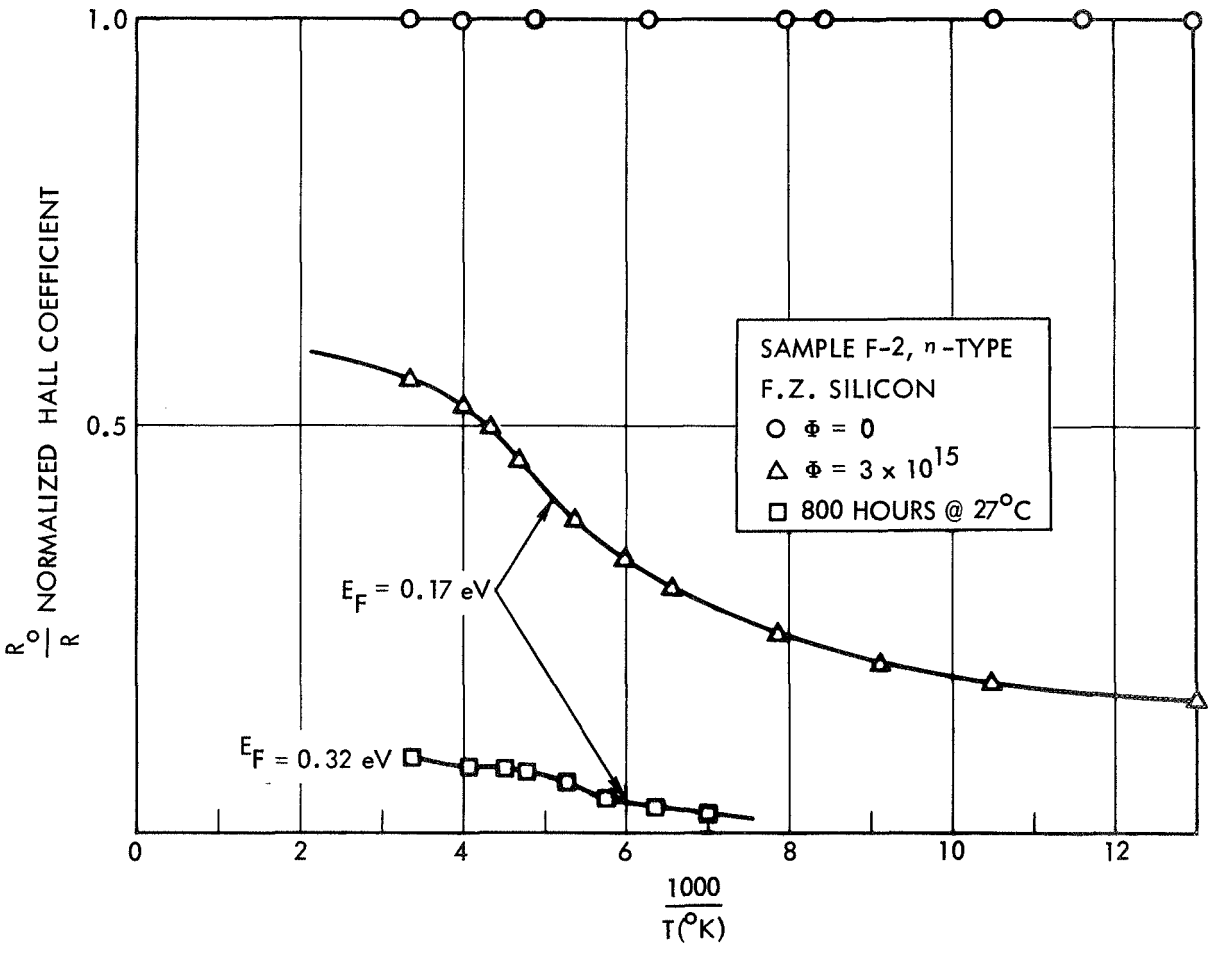

FIG. 3 NORMALIZED HALL COEFFICIENT VS TEMPERATURE, IRRADIATED LI-DOPED FLOAT ZONE SILICON

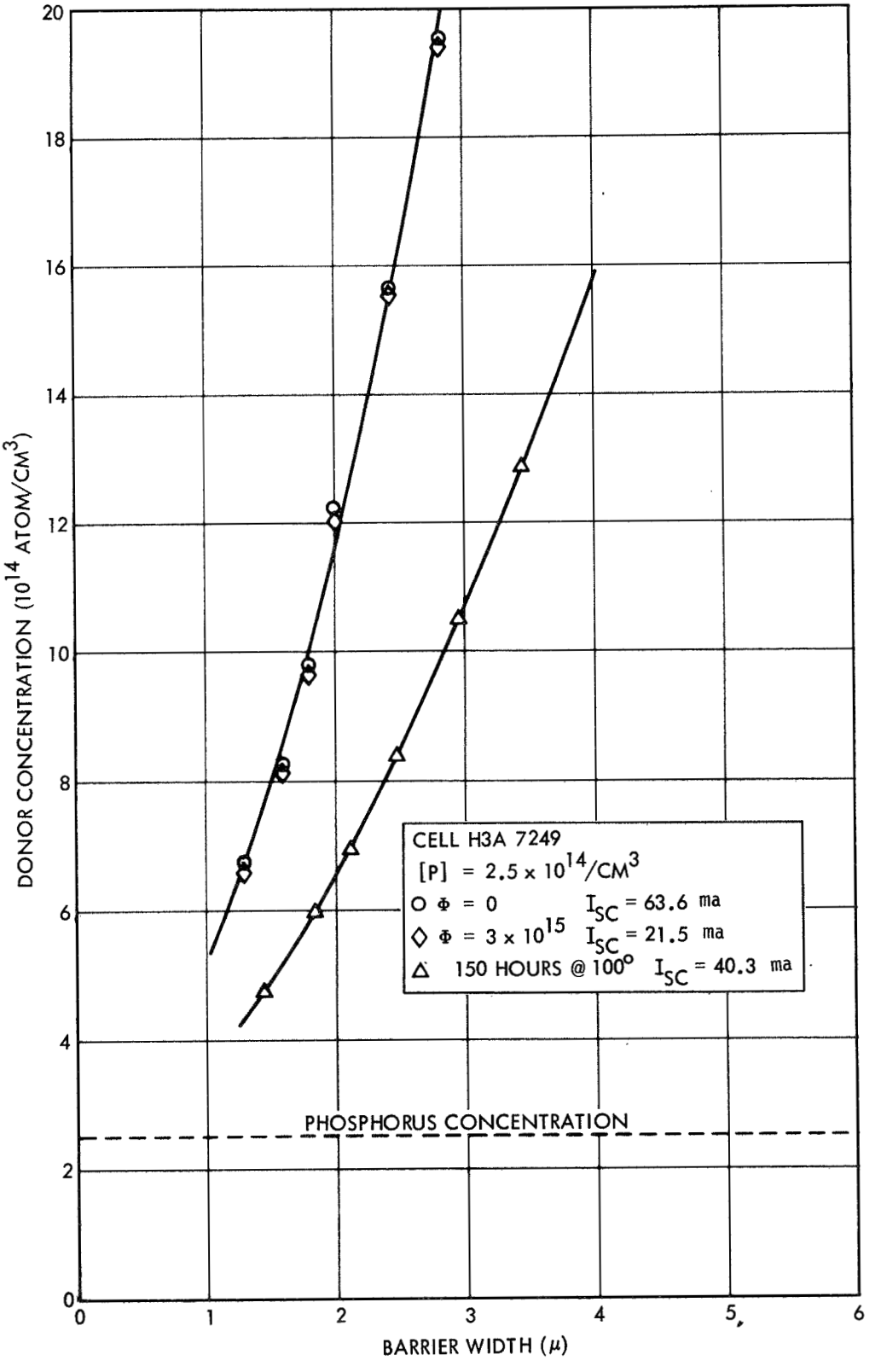

FIG. 4 DONOR CONCENTRATION VS BARRIER WIDTH, CELL H2A 7249

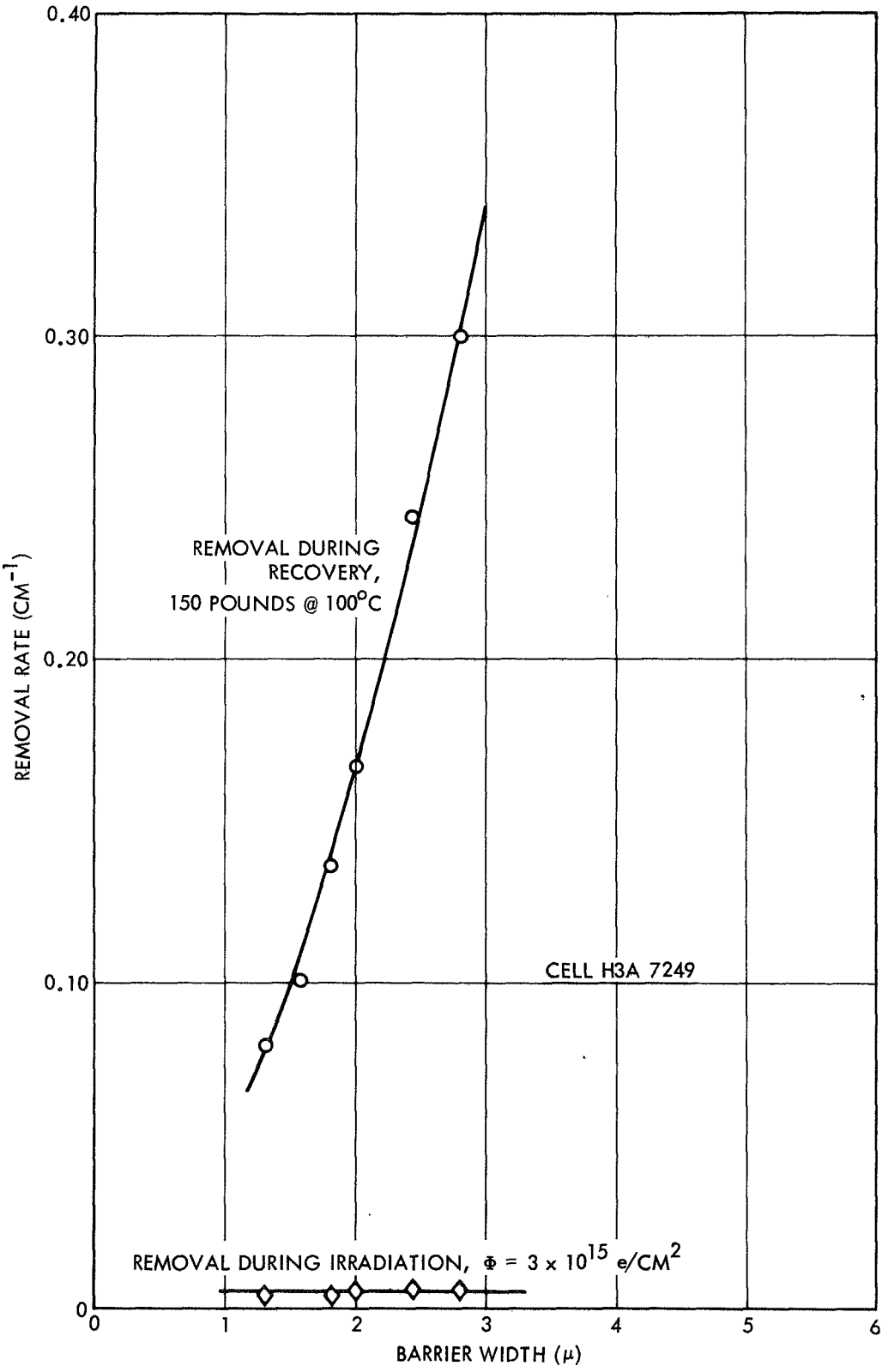

FIG. 5 REMOVAL RATE VS BARRIER WIDTH, CELL H2A 7249

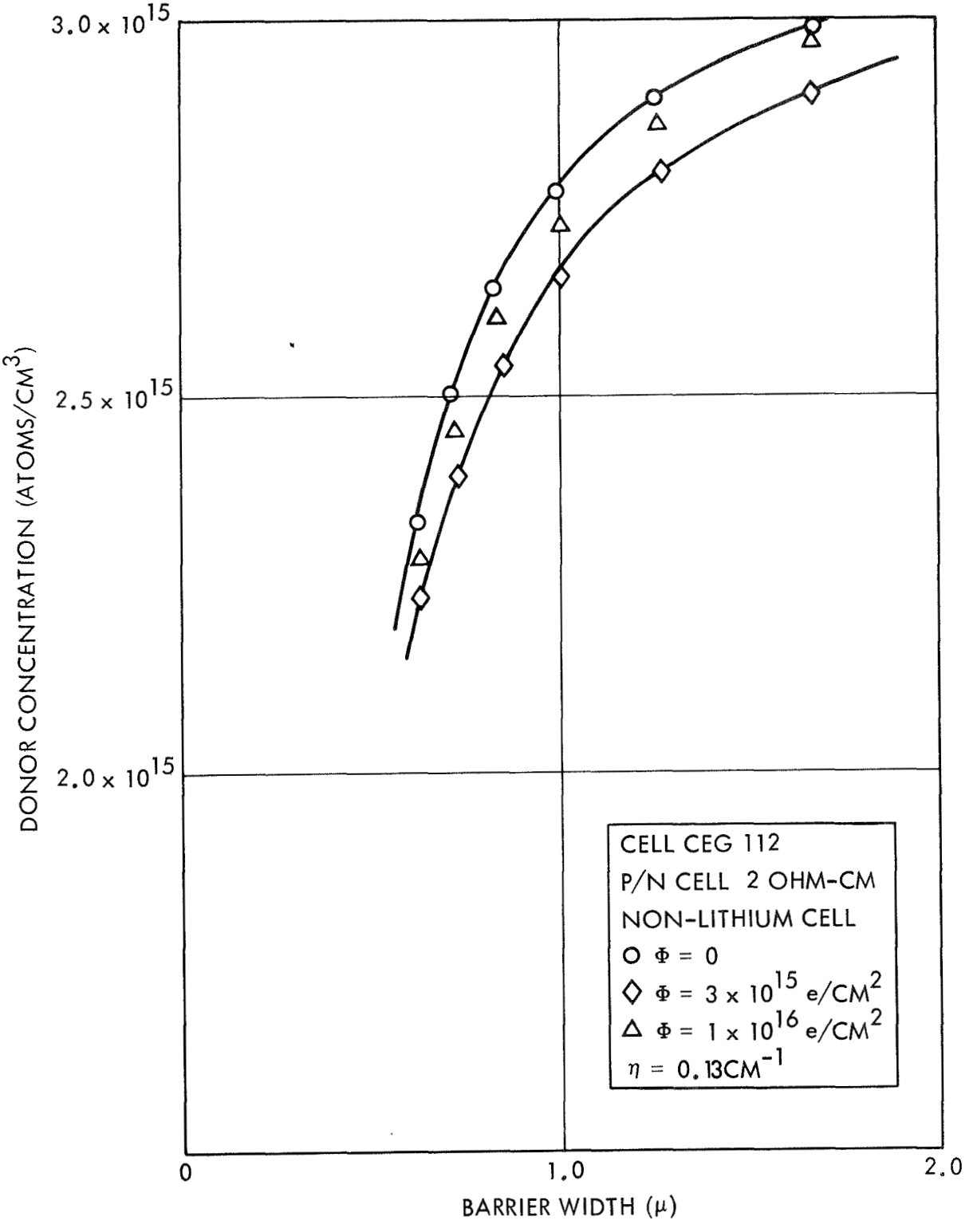

FIG. 6 DONOR CONCENTRATION VS BARRIER WIDTH, CONVENTIONAL P/N CELL

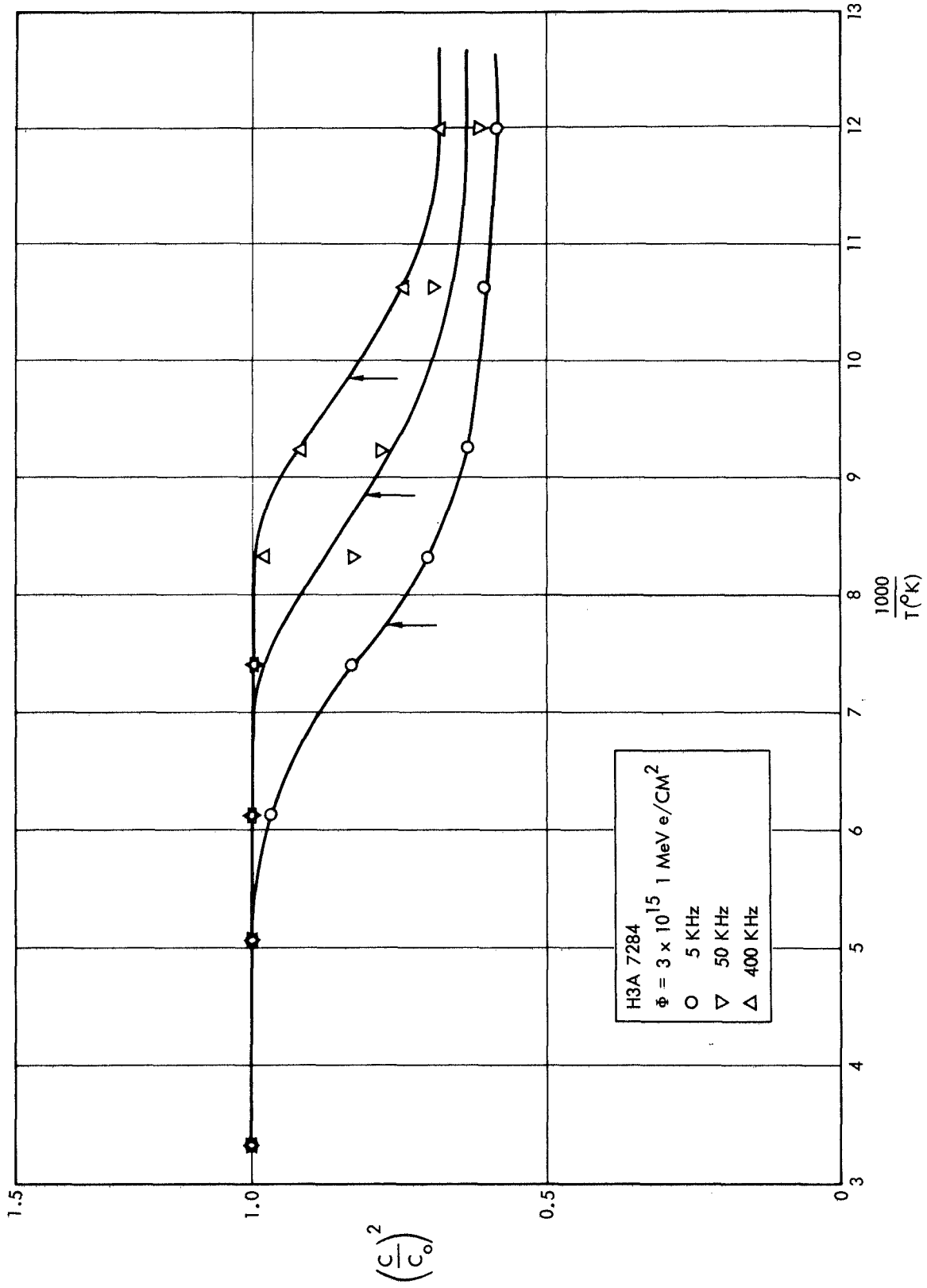

FIG. 7 CAPACITANCE VS TEMPERATURE, VARIOUS FREQUENCIES

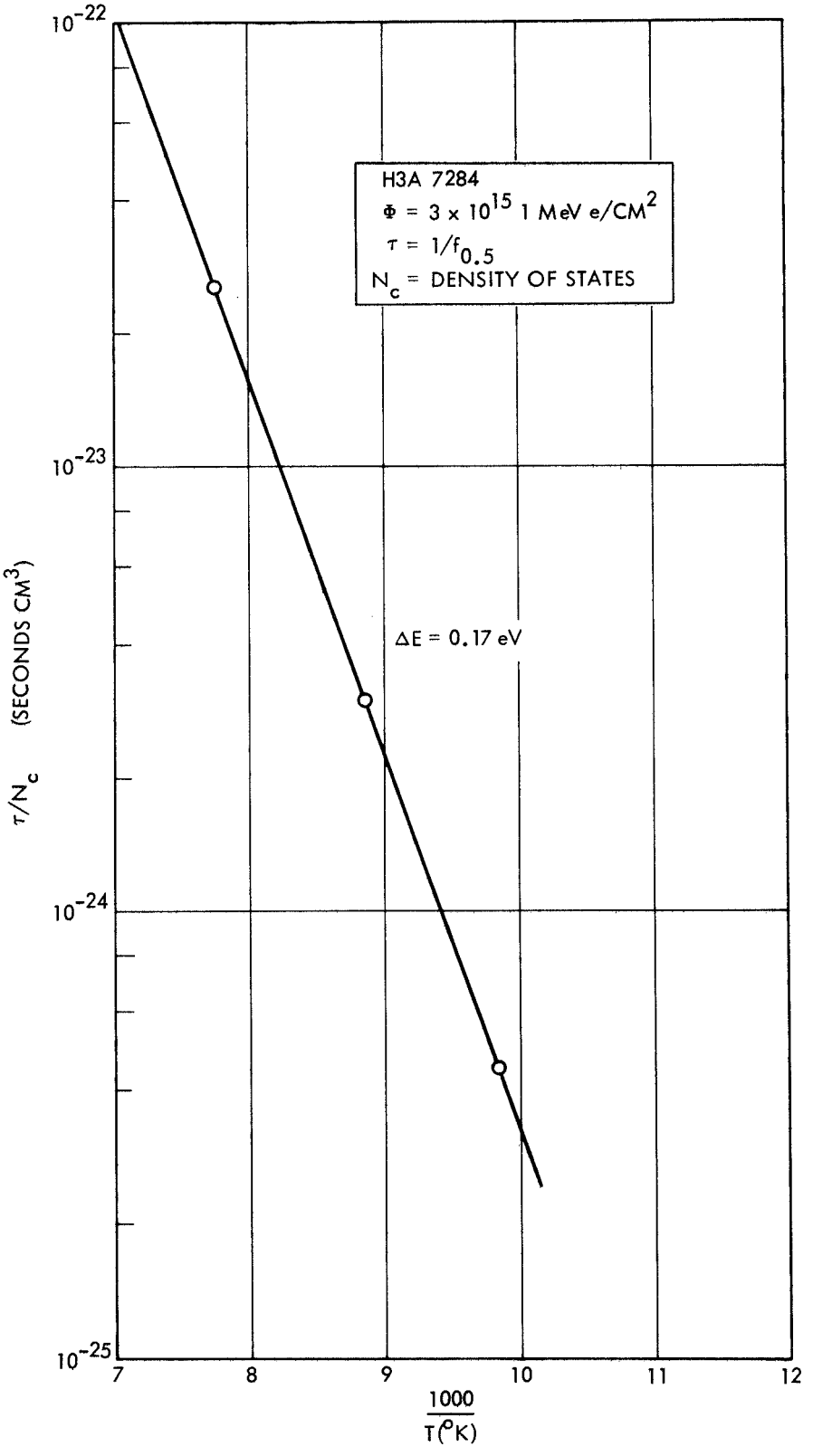

FIG. 8 ACTIVATION ENERGY PLOT, CELL H3A 7284

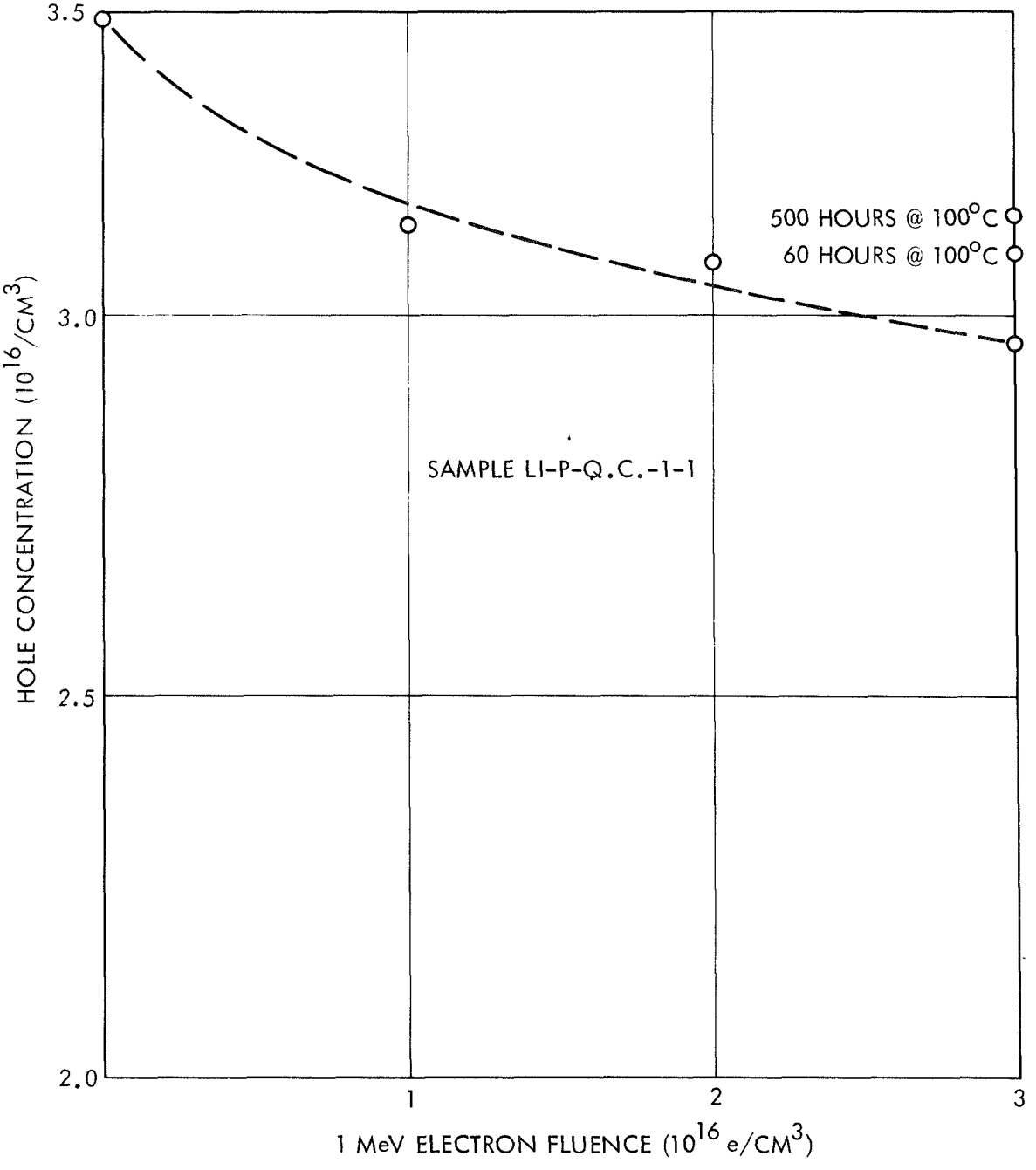

FIG. 9 LITHIUM COMPENSATED P-TYPE SILICON, Q.C.

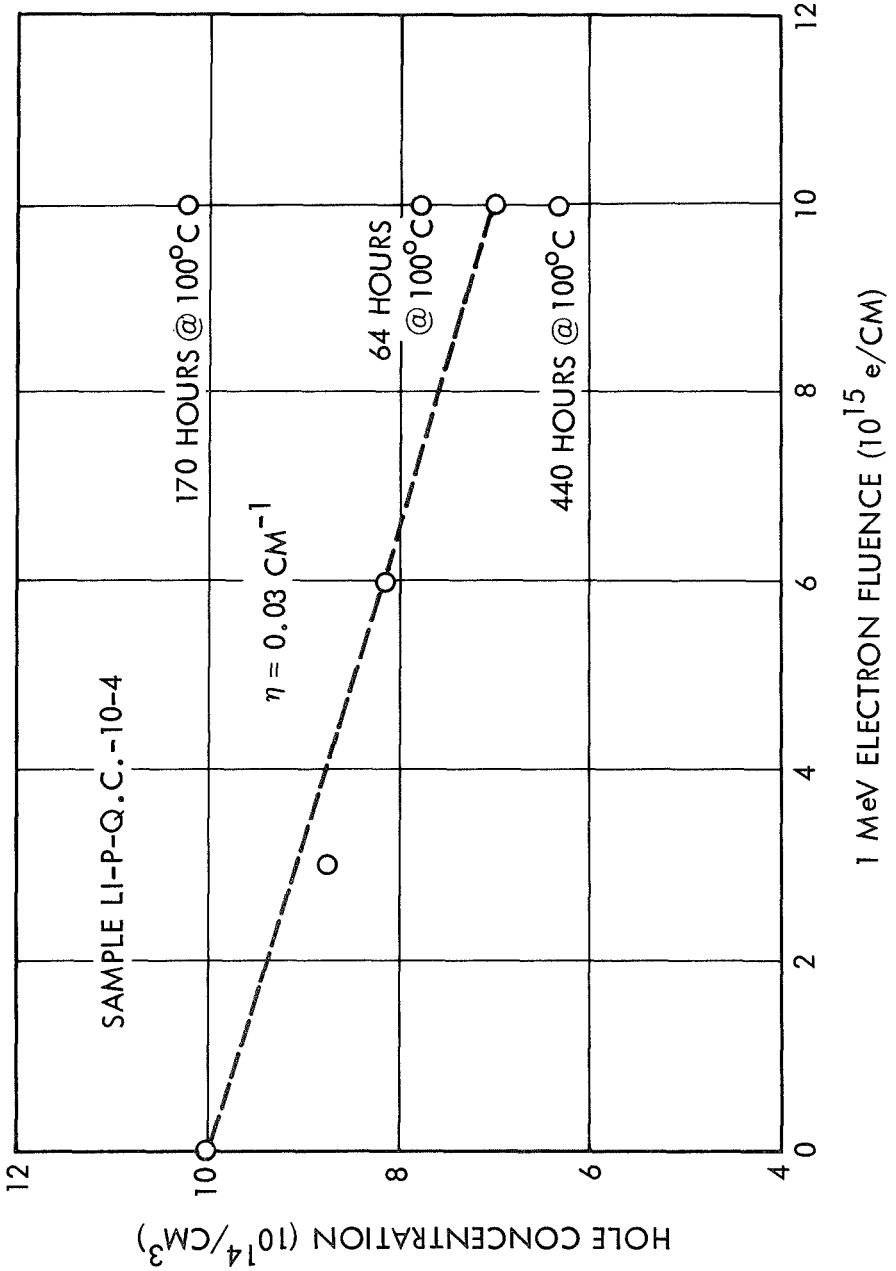

FIG. 10 LITHIUM COMPENSATED P-TYPE SILICON, Q.C.

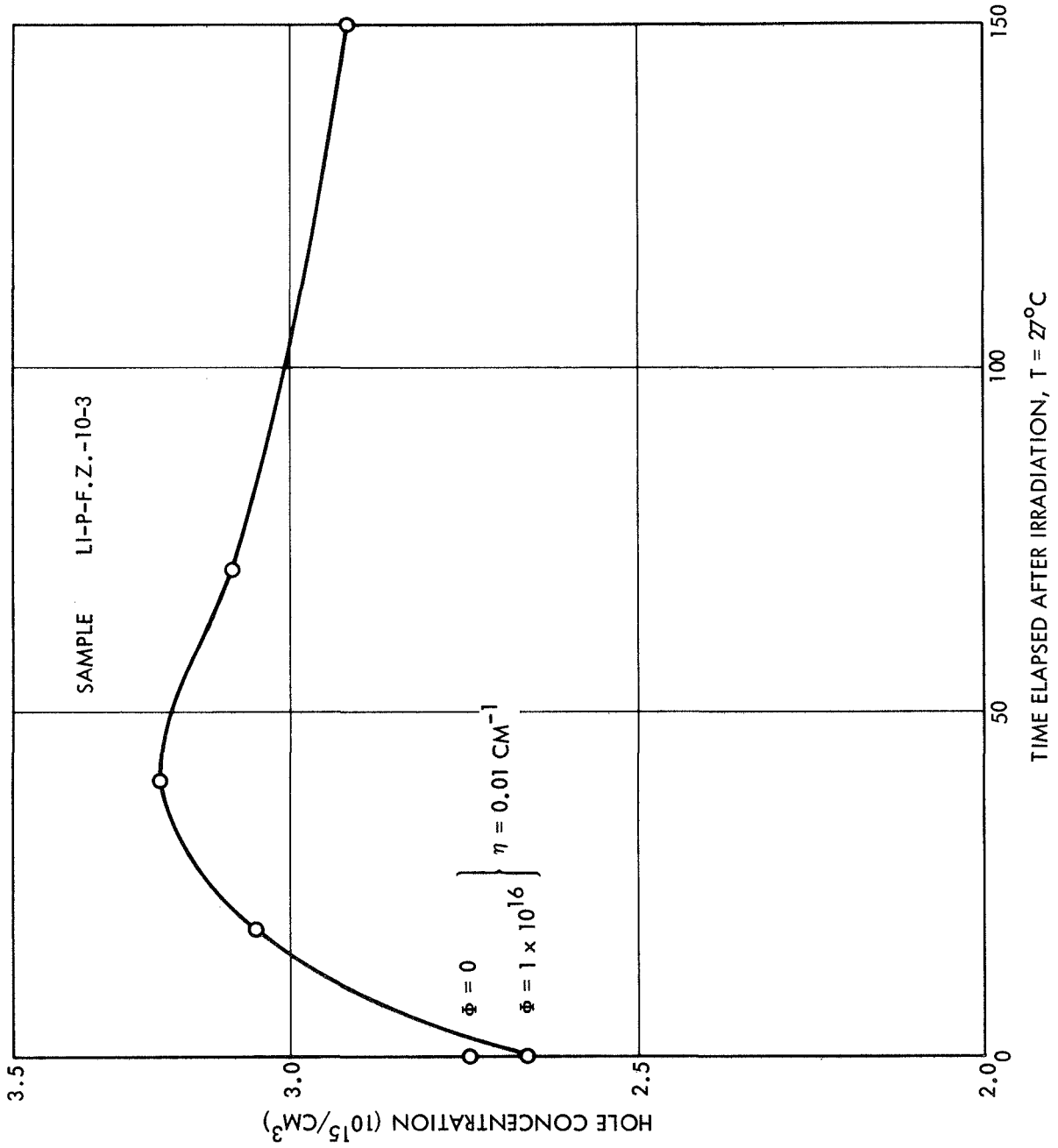

FIG. 11 LITHIUM COMPENSATED P-TYPE SILICON, F.Z.

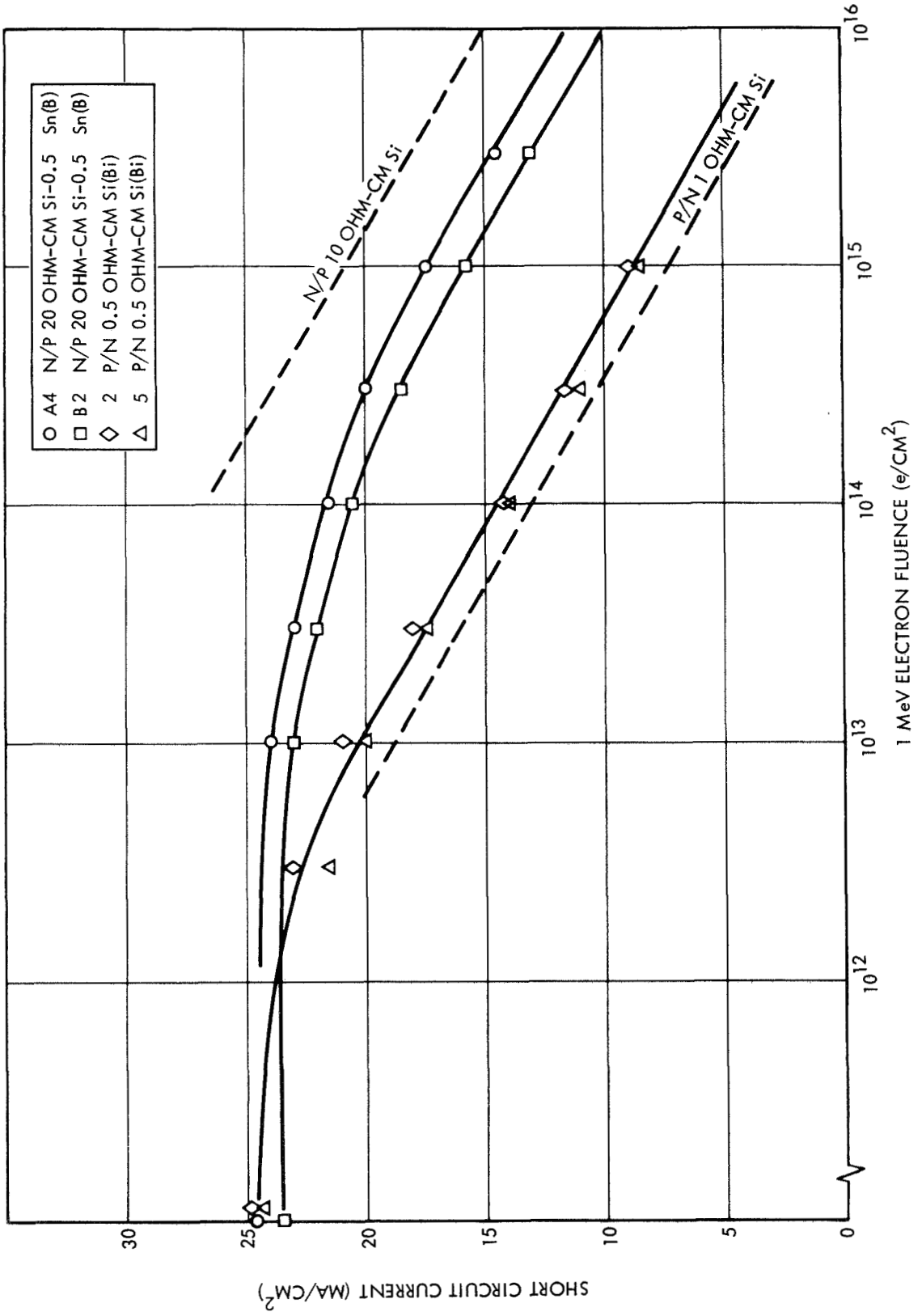

FIG. 12 SOLAR CELLS WITH LARGE SUBSTITUTIONAL IMPURITY ATOMS

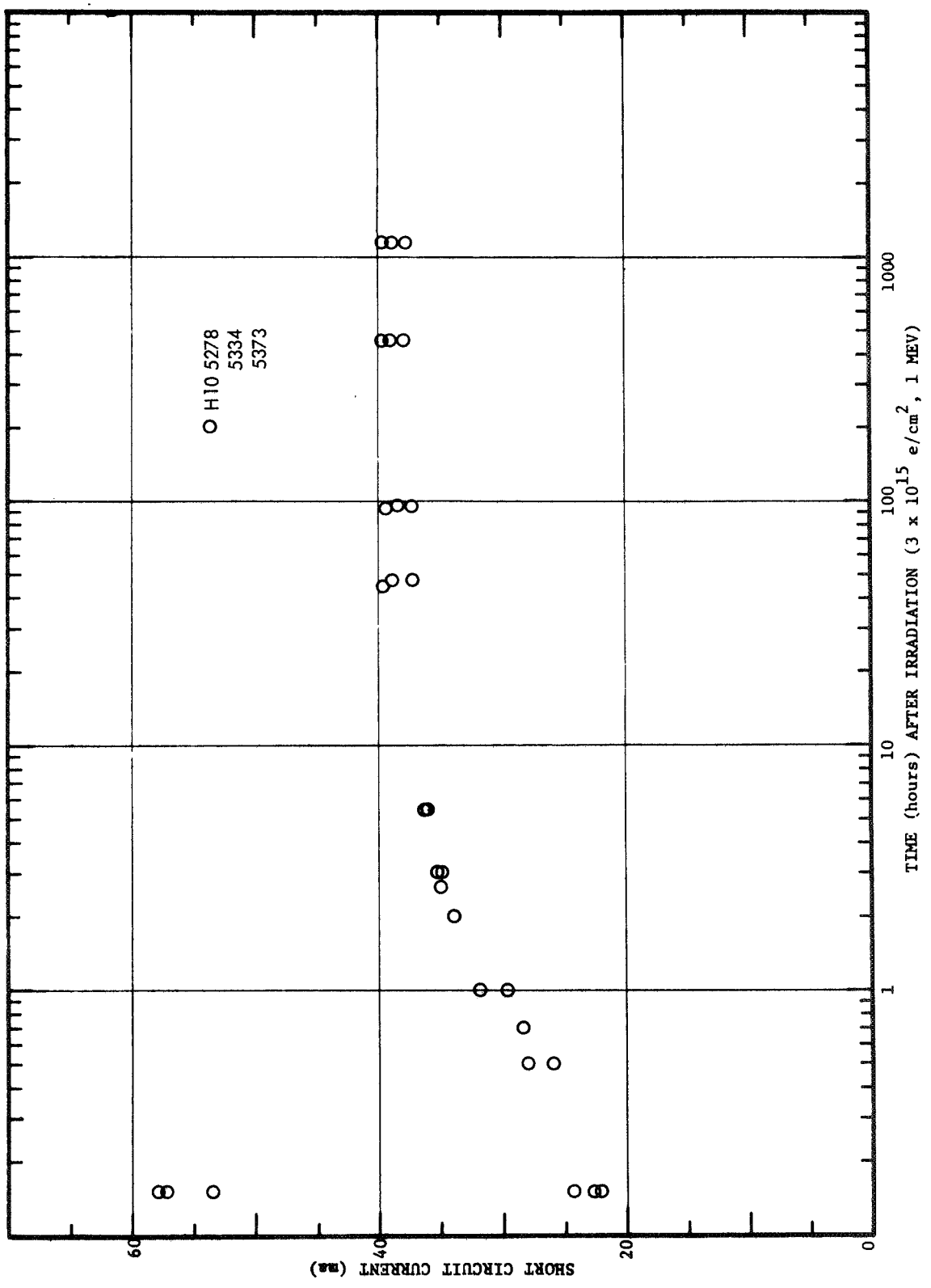

FIG. 13. RECOVERY OF GROUP H10 LITHIUM SOLAR CELLS AT 100°C

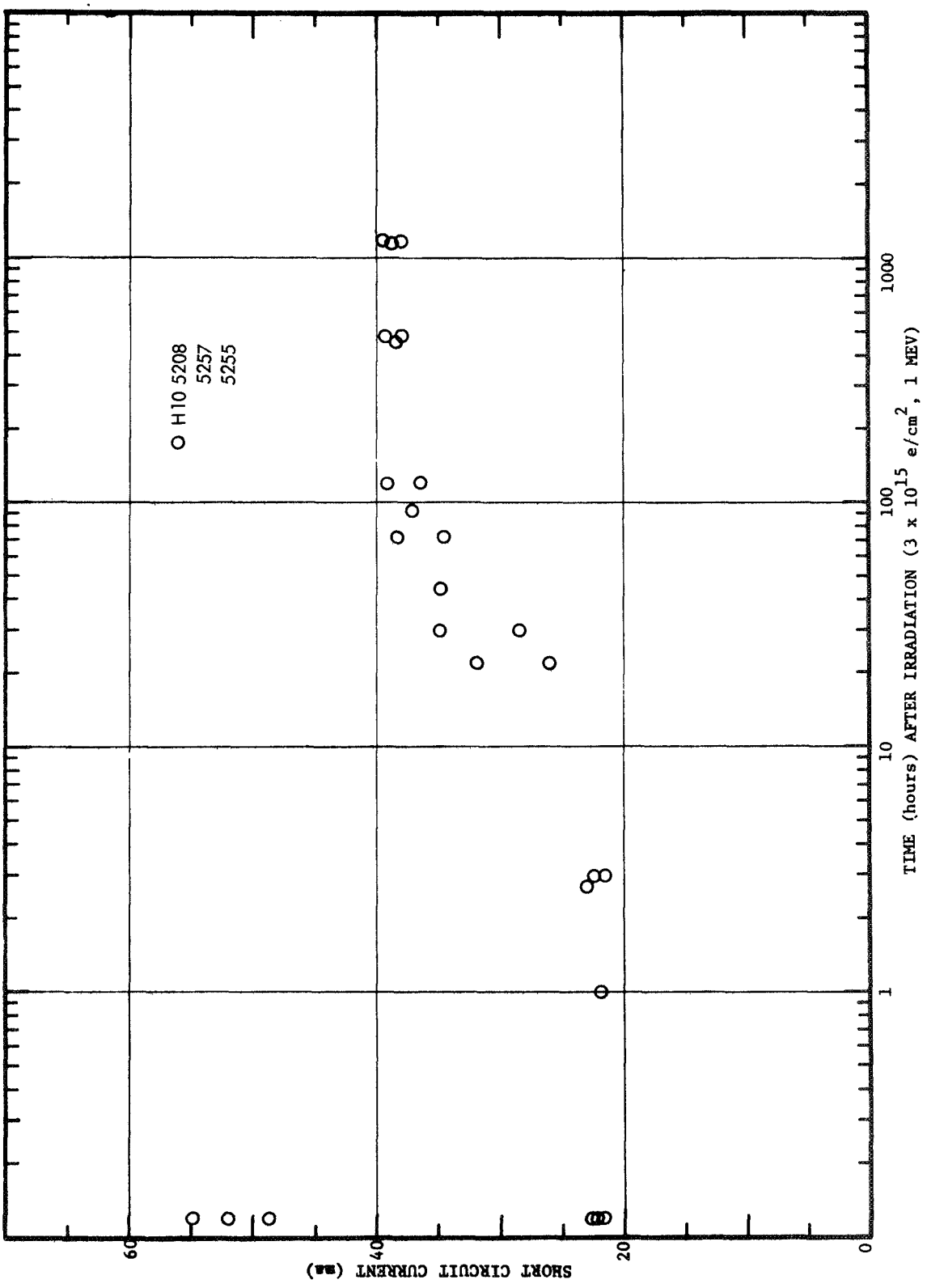

FIG. 14. RECOVERY OF GROUP H10 LITHIUM SOLAR CELLS AT 60°C

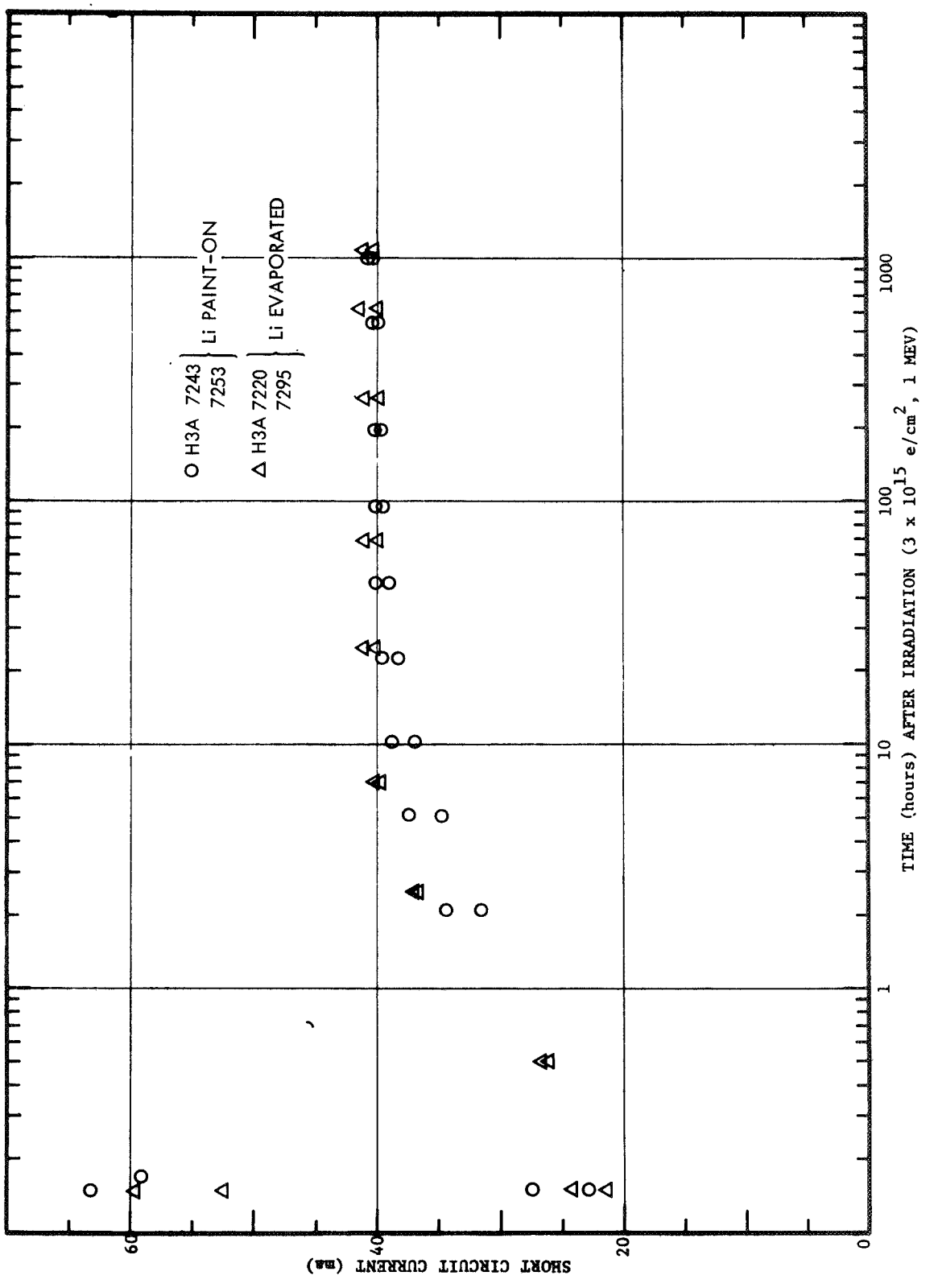

FIG. 15 RECOVERY OF GROUP H3A LITHIUM SOLAR CELLS AT 100°C

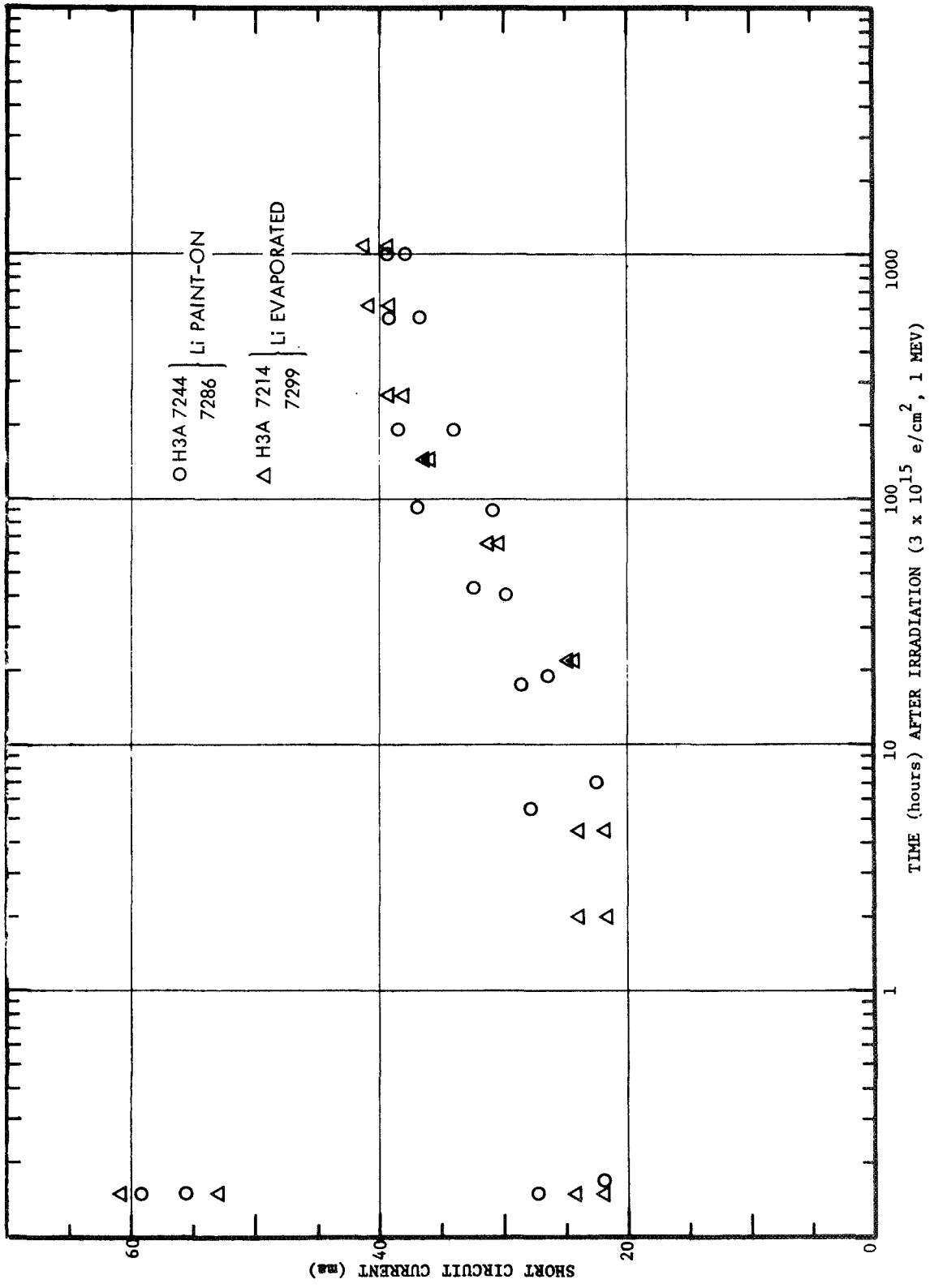

FIG. 16 RECOVERY OF GROUP H3A LITHIUM SOLAR CELLS AT 60°C

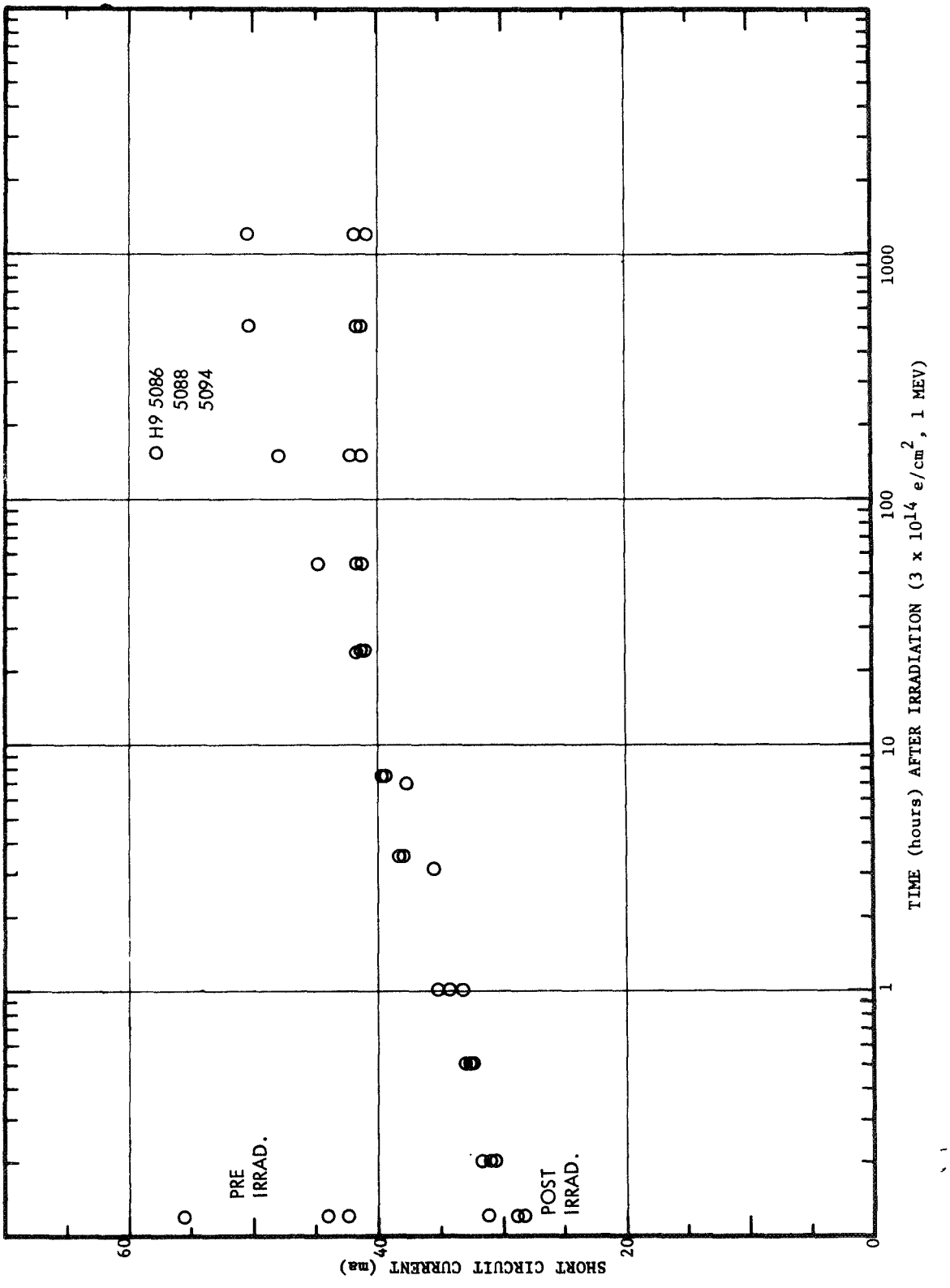

FIG. 17 RECOVERY OF GROUP H9 LITHIUM SOLAR CELLS AFTER $3 \times 10^{14} e/cm^2$

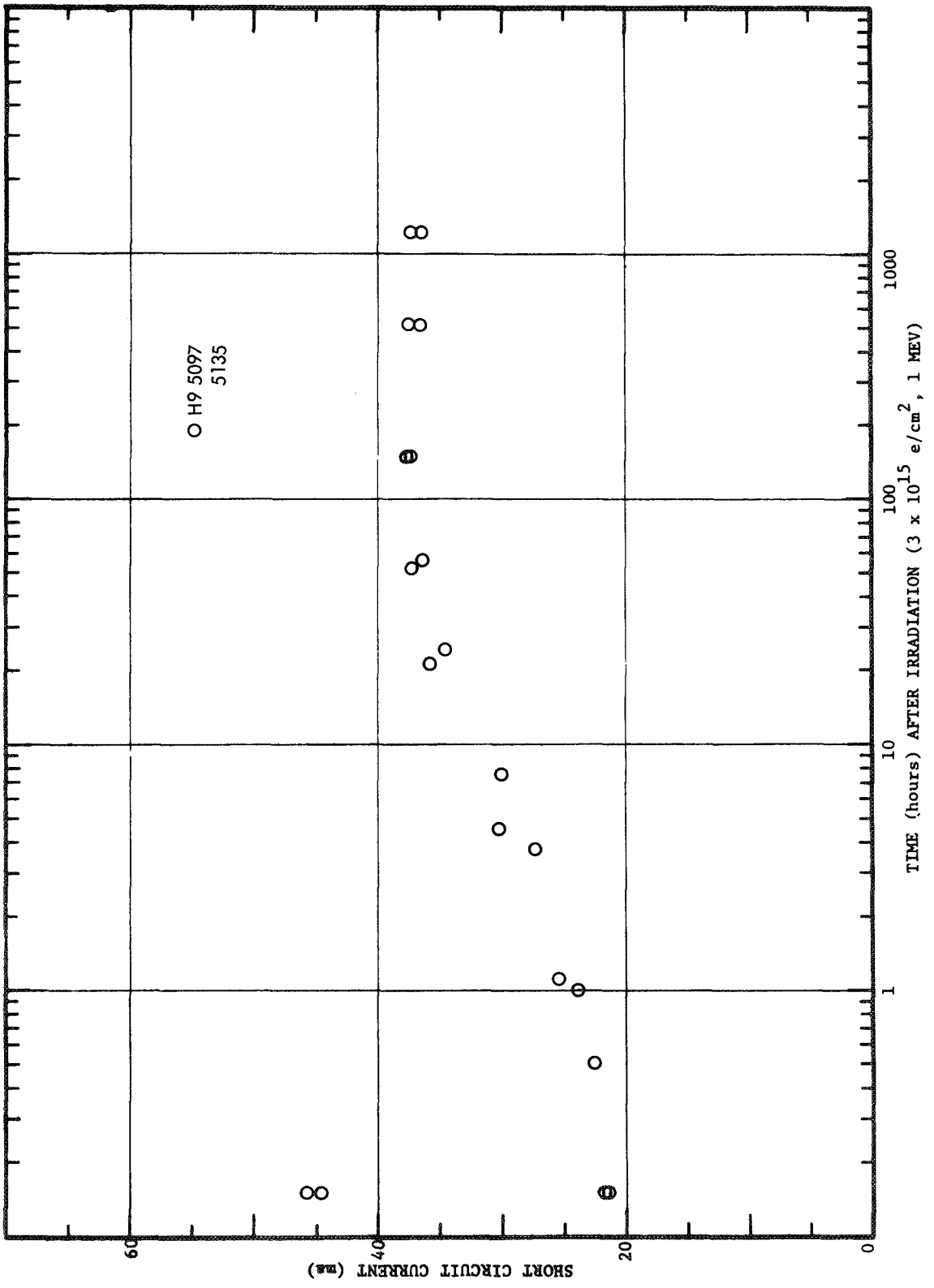

FIG. 18 RECOVERY OF GROUP H9 LITHIUM SOLAR CELLS AFTER $3 \times 10^{15} e/cm^2$

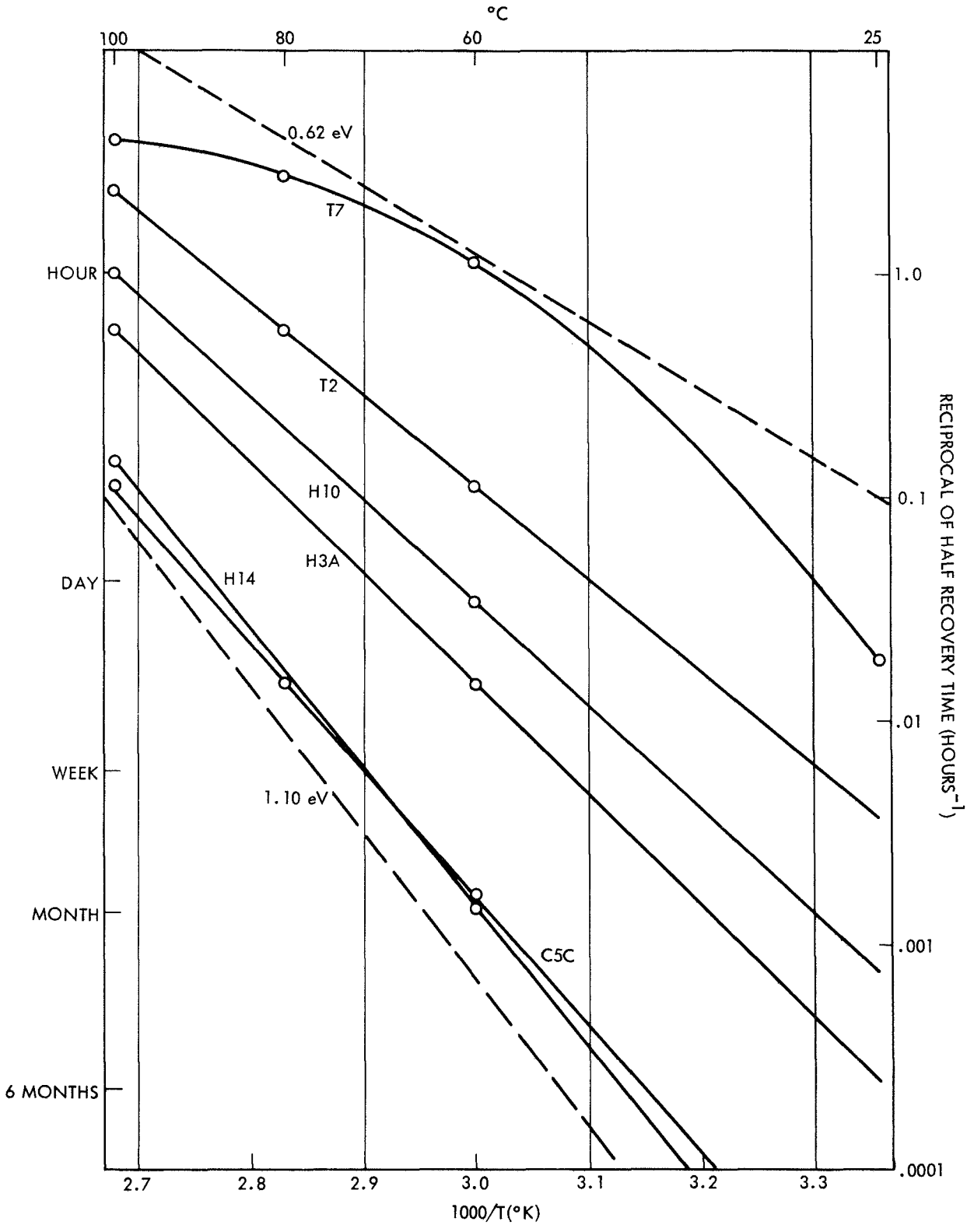

FIG. 19 ANNEALING TIME VS STORAGE TEMPERATURE FOR CRUCIBLE LITHIUM SOLAR CELLS

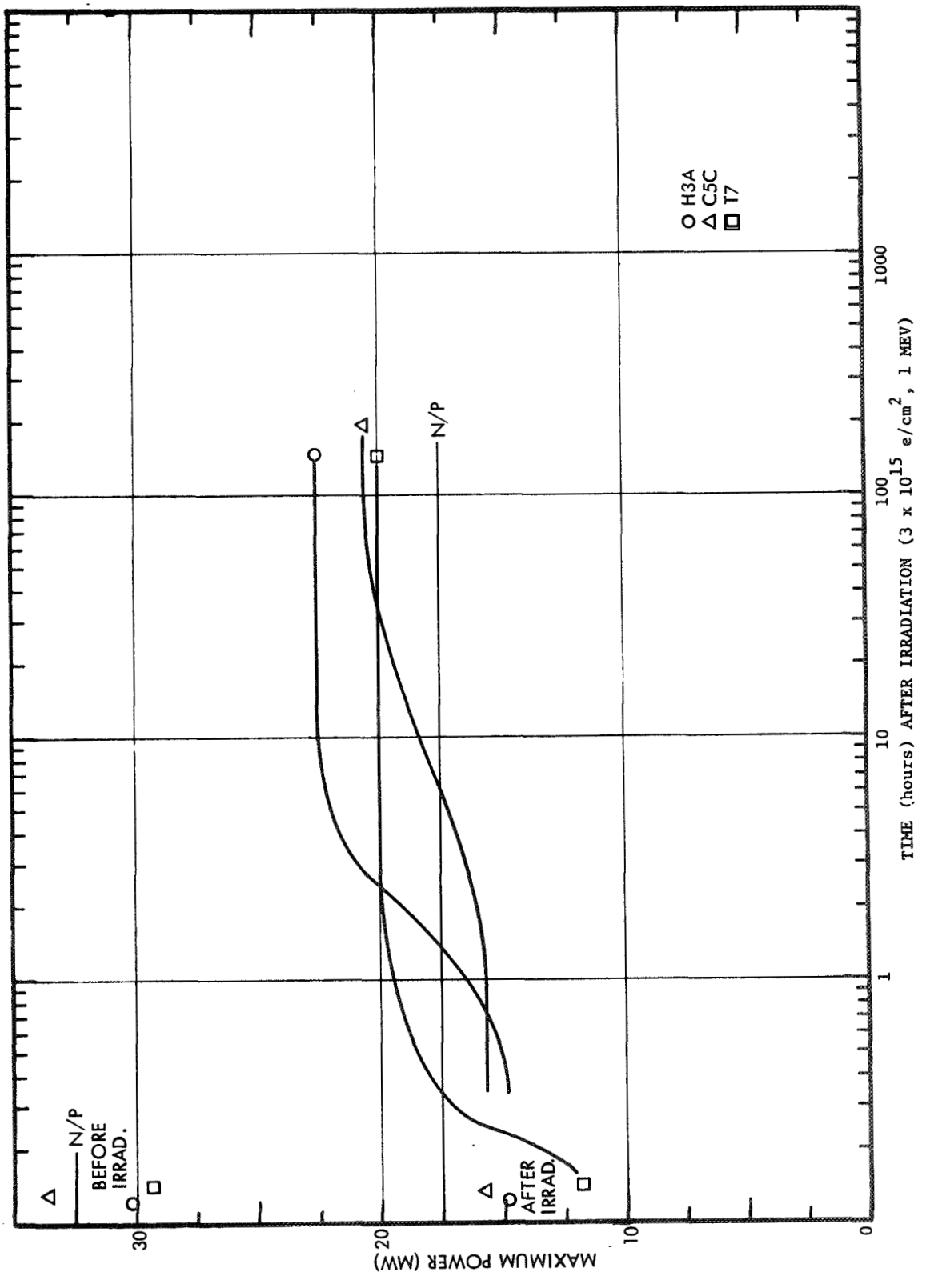

FIG. 20 RECOVERY OF MAXIMUM POWER POINT OF BEST CRUCIBLE CELLS AT 100°C USING SOLAR SIMULATOR ILLUMINATION